

**FINAL REPORT**  
**U.S. Department of Energy**

**Investigation of Novel Electrode Materials for Electrochemically-Based Remediation  
of High- and Low-Level Mixed Wastes in the DOE Complex**

Nathan S. Lewis  
Professor, Division of Chemistry and Chemical Engineering  
Noyes Laboratory, 127-72  
California Institute of Technology  
Pasadena, CA 91125  
Ph: 818-395-6335; FAX: 818-795-7487  
e-mail: nslewis@cco.caltech.edu

Marc Anderson  
Professor of Environmental Engineering  
University of Wisconsin  
Madison, WI 53706  
Ph: 608-262-2674; FAX: 608-262-0454  
e-mail: marc@coefac.engr.wisc.edu

Project Number: 55137  
Grant Number: DE-FG07-96ER14725  
Grant Project Officers: Dr. William Millman & Dr. Romancita Massey  
Project Duration: 10/1/96 to 9/14/00

## Table of Contents

CONTENT	PAGE
Executive Summary .....	3
Research Objectives .....	4
Methods and Results .....	6
Summary .....	14
Electrochemical Studies .....	15
Results	
Characterization of Unsensitized Electrodes .....	18
Spectral Response .....	19
Effect of pH on the TiO <sub>2</sub> Electrochemistry .....	19
Effect of pH on Luminescence of the Adsorbed Dye - TiO <sub>2</sub> / RuL <sup>1</sup> <sub>3</sub> Electrodes .....	20
Summary and Conclusions .....	21
Figure Captions .....	22
Relevance, Impact and Technology Transfer .....	24
Project Productivity .....	25
Personnel Supported .....	25
Publications .....	25
Interactions .....	26
Transitions .....	26
Patents .....	26
Future Work .....	26
Literature Cited .....	26

Feedback ..... 29

**Executive Summary:**

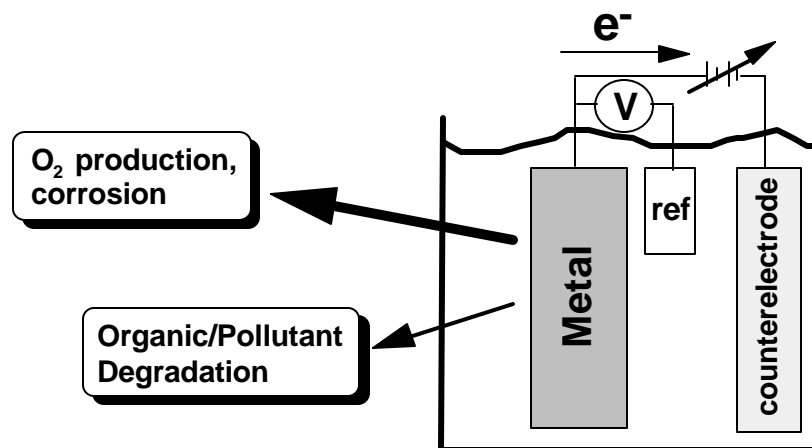
One of the key issues that must be solved to achieve a successful remediation of the high level liquid wastes at the Hanford and at Savannah River sites is the removal of the significant quantities of nitrate and nitrite in the existing liquid waste streams that are presently on these sites in the DOE complex. One method of waste stream remediation is electrochemical oxidation, which is an in-situ method that has been well-documented to have significant advantages in many areas with respect to pump-and-treat approaches to waste remediation. There are, however, significant aspects of the electrochemical oxidation process that need to be addressed from a basic research viewpoint. The research be performed under this proposal has investigated new materials, based on degenerately-doped titanias, for use in the electrochemical degradation of organics and nitrogen-containing compounds in sites of concern to the DOE remediation effort.

## Research Objectives:

To achieve a successful remediation of the high level liquid wastes (HLW) at the Hanford and at Savannah River sites, the significant quantities of nitrate and nitrite must be removed from the existing liquid waste streams that are presently on these sites in the DOE complex. In addition, either prior to or after separation of the high level waste components (for eventual vitrification of the high level components), the Hanford waste stream has a substantial concentration of organics that must be processed in such a fashion that the organics are either removed entirely or are degraded into CO<sub>2</sub> or other benign carbon-containing materials. These process steps are needed so that the low level waste stream obtained after separation of the high level waste components (Cs and Sr, primarily) is suitable for conversion into grout (or possibly vitrified), which is now not feasible due to the high concentration of organic materials currently present in the existing liquid wastes.

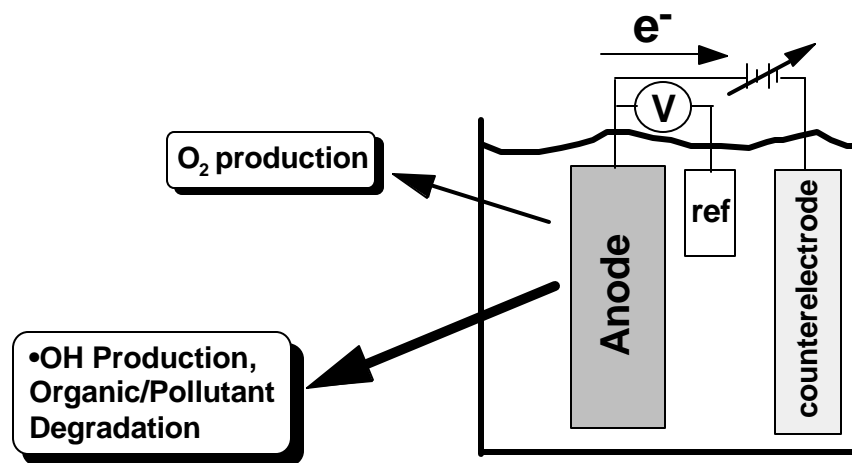
One very promising method of waste stream remediation, which is the focus of this proposal, is electrochemical oxidation. Electrochemical oxidation is well-documented to have some significant advantages relative to high and low temperature steam oxidation processes, including the fact that electrochemical treatment is an in-situ remediation process whereas the water oxidation processes and most other proposed methods are pump-and-treat technologies. In fact, electrochemical degradation of nitrate, nitrite, and organic components in the DOE HLW streams or simulants thereof graded out very highly in a recent DOE assessment of potential remediation methods, with its main drawback relative to high temperature water oxidation processes merely being a lack of prior experience with the operation of electrochemical processes on the scale of, and under the harsh conditions anticipated to be present in, the radioactive waste environment of the DOE sites.

There are, however, significant aspects of the electrochemical oxidation process that need to be addressed from a basic research viewpoint, especially as applied to the unique problems presented by the waste streams in the DOE complex. To date, the electrochemical oxidation process has been investigated primarily using conventional metallic electrodes (Pt, Ni, etc.) or derivatives thereof (Scheme I).<sup>1-4</sup> These metal electrodes can be oxidized, poisoned by contamination, etc., and such processes can be very deleterious to the overall system performance, especially in an environment as complex as that of the HLW streams as presently construed at Hanford and Savannah River. In addition, the metal electrodes waste a great deal of energy, since their faradaic current efficiency for the oxidation of nitrite and organics is low, and a significant fraction of the current is channeled into the well-known, relatively facile oxidation of water to form oxygen gas (or equivalently, hydroxide to oxygen in basic solution) on such surfaces.



**Scheme I.** Electrochemical Oxidation of Organic Pollutants at Metal Electrodes

One approach to circumvent this problem is to utilize alternative, custom-designed anode materials that are likely to have much lower faradaic current efficiencies for water oxidation and therefore to yield much higher energy efficiencies for the desired waste oxidation processes (Scheme II). Such new anode materials would make the electrochemical oxidation method even more attractive if they could be developed and incorporated into a fieldable, practical mixed waste oxidation system. The research to be performed under this proposal will therefore investigate new materials for use in the electrochemical degradation of these organics and nitrogen-containing compounds in sites of concern to the DOE remediation effort.



**Scheme II.** Electrochemical Oxidation of Organic Pollutants  
at Anode Materials Designed to Minimize O<sub>2</sub> Production

## Methods and Results:

### INTRODUCTION

This work is focused on the preparation of novel electrode materials for the degradation of toxic wastes in the DOE complex. One of the goals of this work is to characterize whether it is possible to use controlled doping of  $\text{TiO}_2$  with species such as Nb in order to create new electrode materials that will facilitate the destruction of undesirable organics and inorganics, without light and instead only with an applied potential, in the waste tanks at the DOE sites. In the first part of this project, we have therefore spent an extensive amount of effort characterizing, as a baseline, the chemical and electrochemical behavior of  $\text{TiO}_2$  itself, so that we can make robust comparisons to the behavior of the Nb-doped systems in subsequent work on this project. The preparation of these electrode films is being performed by Marc Anderson at Wisconsin, who is preparing a number of different stoichiometries, grain sizes, etc. for investigation of their electrochemical properties by the Lewis group at Caltech. First we report on the progress of the electrode preparation work, and then we describe progress on the electrochemical work.

Several types of metallic supports have been coated with suspensions of various metal oxides. In this report, we describe studies in which titania has been coated on copper, aluminum, stainless steel, and titanium supports for further testing in photoelectrocatalytic systems.

### EXPERIMENTAL

#### Reagents

All chemicals (Aldrich Chemical Co. and Fisher Scientific Co.) were used without further purification. The water was deionized using a Barnstead NANO pure UV ultrapure water system.

#### $\text{TiO}_2$ Sol Preparation and Characterization

Sol-gel processing techniques were employed to prepare three different titania sols (two aqueous-based and one alcoholic-based) for use in this study.<sup>5,6</sup> An aqueous-based sol was prepared by mixing  $\text{H}_2\text{O}$ , titanium isopropoxide ( $\text{Ti}(\text{i-OPr})_4$ ) and conc.  $\text{HNO}_3$  in a volume ratio of 300/24.75/2.1 with rapid stirring at room temperature. The resulting precipitate of titania was peptized by continuing to stir for 3 days until a stable suspension was obtained. This acid suspension was then dialyzed to a pH of 3.5.<sup>7</sup>

Another aqueous-based sol was prepared by mixing  $\text{H}_2\text{O}$ ,  $\text{Ti}(\text{i-OPr})_4$  and conc.  $\text{HNO}_3$ , in a volume ratio of 300/30/2, with rapid stirring at room temperature; the resulting precipitate was peptized by refluxing the mixture at  $80^\circ\text{C}$  for three days.<sup>7</sup> This aqueous sol was used only to coat some samples of 304 stainless steel.

In addition, an alcohol-based sol was prepared. An alcohol exchange reaction was employed to convert  $\text{Ti}(\text{i-OPr})_4$  to the tertiary amyl alcohol (t-AmOH) analogue.<sup>8</sup> The titania sol was then prepared by adding, with stirring, a solution of 0.72 ml of water in

49.28 mL of t-AmOH to a solution of 9.32 mL of  $\text{Ti}(\text{t-OAm})_4$  in 40.68 mL of t-AmOH at room temperature.

Xerogels of the aqueous based sol were prepared by allowing the solvent to evaporate slowly at room temperature. Porosities and surface areas of the unsupported xerogels after firing at different temperatures were determined by BET analysis of nitrogen adsorption isotherms. The particle size distribution in both sols was measured by laser light scattering (Brookhaven Instruments Corp.).

### TiO<sub>2</sub> Thin-Film Preparation and Characterization

Plates of copper, aluminum, 304 stainless steel and titanium (Goodfellow Cambridge Limited) measuring 50x100x0.5 mm were prepared. Copper and aluminum plates were cleaned by placing them in acetone in an ultrasonic bath for 15 min. Titanium and stainless steel plates were first polished with Hope's stainless steel polish (The Hope Company, Inc., Bridgeton, MO). These plates were then cleaned ultrasonically with acetone as explained above. The final steps in preparing the titanium plates were to dip them in hot 50 vol% hydrochloric acid for 2 min and rinse them with MilliQ water.

Aluminum, copper and titanium plates were dip-coated (withdrawal speed: 1.5 cm min<sup>-1</sup>) with a single layer of the alcohol-based sol and fired at 450 °C for 1 h. Coated copper plates were not treated further. Coated aluminum and titanium plates were dip-coated a second time (at the same withdrawal speed) with a single layer of dialyzed aqueous-based TiO<sub>2</sub> sol and fired at either 300, 400 or 500 °C for 5 h. In some cases this procedure was repeated to deposit more layers of TiO<sub>2</sub>.

Stainless steel plates were first fired at 450 °C for 2 h, in order to produce a metal oxide film that improved the adherence of the titania coating to the substrate.<sup>9</sup> These pre-treated plates were dip-coated (same withdrawal speed) with one layer of the dialyzed aqueous-based sol and fired at either 300 or 500 °C for 2 h. In some cases this procedure was repeated to deposit more layers of TiO<sub>2</sub>.

In order to study the inhibition of corrosion, samples of bare stainless steel were fired 450 °C for 2 h, after which they were coated with several layers of the various titania sol and, then fired at 500 °C for 5 h. One additional sample, coated with the sol that was peptized at 80 °C, was fired at 700 °C for 5 h.

The surfaces of these photoelectrodes were characterized with scanning electron microscopy (SEM), while the crystal structure of the deposited coatings was determined by X-ray diffraction (XRD) analysis of the film.

### Reactor System and Auxiliary Equipment

Studies were conducted in a batch reactor system whose principal components were a borosilicate glass rectangular reactor vessel 55x66x25 mm (Vitro Com Inc., Mountain Lakes, NJ), placed 10 cm in front of a 15 W fluorescent ultraviolet bulb (General Electric,

F1ST8.BLB). The reactor and the lamp were placed in a black acrylic box in order to avoid extraneous illumination. A plastic cap was placed on the reactor in order to seal it and hold three electrodes. Initially, 70 mL of test solution was put in the reactor, which allowed 25 cm<sup>2</sup> of the supported TiO<sub>2</sub> film to be immersed into the solution. The intensity of light striking the electrode was 1.35 mW cm<sup>-2</sup>, as measured by a photometer (International Light Inc., Model IL 1400A). Electrical potentials in the reactor were controlled by a potentiostat (IBM, EC/225) that was connected to a counter electrode (platinum mesh 20x50 mm), a working electrode (metal-supported TiO<sub>2</sub> film), and a reference electrode (saturated calomel). All potentials are reported relative to that of the saturated calomel electrode.

### Photoelectrocatalytic Reactions

The photoelectrocatalytic degradation of formic acid was conducted in the reactor system described above. Given potentials were applied with the three electrode system to perform photoelectrocatalytic reactions. Tests were conducted using aqueous solutions of formic acid (25 ppm as C) in 0.01 mol dm<sup>-3</sup> NaCl. Oxygen was bubbled through the test solutions during all reactions. In each experiment two samples were taken at a given time; the first set of samples was obtained 15 min after the UV light was turned on (to allow the system to stabilize), while the second set of samples was obtained three hours after the UV light was turned on. In order to characterize the behavior of the titania coatings that were placed on various metallic electrodes, two properties of these photoelectrodes were monitored. One property was the photocatalytic activity of the electrode under set operating conditions. This property was measured by determining the percentage of degradation in each experiment as calculated from the change in the average concentration of total organic carbon (TOC) in each sample after illumination for 3 h. TOC values were measured with a TOC analyzer (Shimadzu Instruments, Model TOC 5000). A second property of interest was the stability of the photoelectrodes. This property was determined by measuring the photocatalytic activity of each photoelectrode, at least three separate times, at an applied potential of +0.5 V (vs SCE), and noting if any changes in activity occurred in the different measurements over time.

## RESULTS

### Stability and Activity of Copper-Supported Photoelectrodes

To date all the attempts to produce a stable coating of titania on a copper plate have been unsuccessful. It appears that a layer of CuO forms underneath the coating of titania. This layer of CuO readily delaminates during testing, resulting in the loss of the titania coating.

### Stability and Activity of Aluminum-Supported Photoelectrodes

TiO<sub>2</sub> supported on aluminum displays photocatalytic and photoelectrocatalytic activity, but the TiO<sub>2</sub> coated aluminum electrodes corrode after several hours of use. Scanning electron micrographs of these photoelectrodes indicate that the TiO<sub>2</sub> coating is deposited uniformly on the aluminum surface before use (see Figure 1a). However, after use, much of the TiO<sub>2</sub> coating has delaminated from the substrate, and the substrate itself displays

significant amounts of pitting and corrosion (Figure 1b). The application of a positive potential across the photoelectrodes accelerates the corrosion process and Al(III) is released to the solution. For example, when +0.30 V were applied across a TiO<sub>2</sub> coated aluminum electrode, 101 ppm of Al (III) were found in the solution after 12 h of treatment.

Corrosion was observed when the bare aluminum substrate was placed in contact with the test solution (25 ppm, as C, formic acid in 0.01 mol dm<sup>-3</sup> NaCl) in the presence of O<sub>2</sub> and UV light (Figure 1c). The corrosion of these electrodes was so severe that it could be observed visually. The extent of corrosion may be related to the test solution being treated. Less corrosion might be observed if less aggressive test solutions were employed. Thus it appears that Al-supported TiO<sub>2</sub> electrodes are not suitable for this application. No further studies were conducted with this system.

### Stability and Activity of Stainless Steel-Supported Photoelectrodes

Photomicrographs of the surfaces of the fired 304 stainless steel plates (304 SS) before coating indicate that these surfaces are covered by numerous fine particles (ca. 100 nm diameter). The source of these particles has not been identified. They could be either material that was deposited while polishing these plates or small iron oxide particles formed on the surface. When the surface of the stainless steel is coated with an aqueous-based dialyzed sol of TiO<sub>2</sub>, the resulting film follows the contours of the surface of the metal and covers the particles that are present on that surface. These coatings are quite thin; a coating prepared by depositing two layers of alcohol-based sol and firing at 500 °C for 5 h was less than 100 nm thick (see Figure 2). TiO<sub>2</sub> supported on stainless steel electrodes has been used previously to study the purely photocatalytic degradation of formic acid and malic acid.<sup>9,10</sup> We employed this material to study both photocatalytic and photoelectrocatalytic processes.

When the photoelectrodes prepared for this study were tested for purely photocatalytic activity (i.e. no applied potential), such activity was observed. An average of 5.5% of the initial formic acid present in the solution was degraded in a three hour period, when a photoelectrode coated with one layer of the dialyzed aqueous TiO<sub>2</sub> sol and fired at 300 °C was used. When an electrode with 6 layers of dialyzed aqueous TiO<sub>2</sub> sol that was fired at the same temperature was used, the percentage degraded in the same period was 30%. Photomicrographs of the surface indicate that no observable change occurred during these tests. In the case of an electrode coated with one layer of dialyzed aqueous TiO<sub>2</sub> sol and fired at 500 °C, only 1% of the initial formic acid was degraded in three hours.

However, when the same electrodes were employed as photoanodes, they were observed to corrode under applied potentials more positive than 0.0 V. The corrosion was obvious, because the oxidized iron caused the test solution to turn red-orange.

In an attempt to prevent the dissolution of the metallic substrate by isolating the stainless steel from the solution, additional samples coated with each type of the different TiO<sub>2</sub> sols described previously were applied. 304 SS plates were coated with 1, 2 and 3 layers of each of the sols (each plate always being coated with the same sol) and fired at 500 °C for 5 h after each layer was applied. The stability of the samples to applied positive

potentials was tested by measuring current vs. applied potential. These experiments were conducted in the dark using a Teflon cell. Titania-coated stainless steel electrodes were used as working electrodes with a platinum counter electrode and SCE reference electrode. The cell was filled with a working solution of 25 ppm (as C) formic acid in  $0.01 \text{ mol dm}^{-3}$  NaCl. The potential was scanned at  $20 \text{ mV s}^{-1}$ .

In all tests, a large increase in current was observed when the applied potential exceeded 50 mV, as shown in Figure 3. In addition, the surface of the electrode that was in contact with the solution looked damaged after 5 cycles from 500 mV to -500 mV. However, SEM images do not show any differences between the areas of the electrodes that contacted the test solution and the areas that were not exposed to the solution.

Figure 4 presents SEM images of the surfaces of the 304 SS electrodes either bare or coated with the different sols. Figure 4a shows the surface of a 304 SS plate that was fired at  $500 \text{ }^\circ\text{C}$ . This figure indicates the presence of the small particles (ca 100 nm) previously described. Figure 4b is a magnification of the previous image in which some of the particles are shown. Figure 4c shows the surface of an electrode coated with three layers of the alcohol-based sol, in which the typical particles present on the surface of the 304 SS after firing can be seen. Figure 4d is a magnification of the previous image. This view shows that the particles present on the surface (light grey) are now coated by smaller particles of  $\text{TiO}_2$  (ca 20 nm). Figure 4e shows the surface of an electrode coated with one layer of the dialyzed aqueous sol. This film is thin enough that particles and some scratches on the surface are visible through the film. Figure 4f is a magnification of the previous view. The particles of  $\text{TiO}_2$  deposited from the dialyzed aqueous sol are larger and less uniformly distributed than the particles deposited from the alcoholic sol.

Figure 4g shows the surface of an electrode coated with one layer of the aqueous sol peptized at  $80 \text{ }^\circ\text{C}$ . In this case, the film appears to completely cover the particles on the surface. Therefore, we believe that this film is thicker than the others, which is a consequence of the higher viscosity of this sol compared with the others. In fact, this film is so thick that it delaminates from the electrode in several areas (not shown in the photograph). Figure 4h is a magnification of the previous image which shows the arrangement of the particles in this film.

One plate was coated with a layer of the aqueous sol peptized at  $80 \text{ }^\circ\text{C}$  and fired at  $700 \text{ }^\circ\text{C}$  for 5 h. The voltammograms obtained with this electrode were identical to that shown in Figure 3; and, after 50 cycles, the surface again appeared damaged. As can be noticed by comparing Figures 5a-d to Figure 4, this surface appears quite different than the films obtained by firing at  $500 \text{ }^\circ\text{C}$ . The uncoated area is covered by small crystals (100-200 nm) in a compact arrangement (see Figure 5a). However, the coated areas contain relatively large structures on the surface (see Figure 5b) whose composition is mostly iron oxide, as determined by energy dispersive X-ray spectroscopy (EDX) analysis. (The particles shown in Figure 6a are too small to provide useful information using this technique). The morphology of these structures appears to be a compact arrangement of deformed monocrystals (see Figure 5c). The presence of these iron oxide structures on the surface indicates that the  $\text{TiO}_2$  coating cannot prevent corrosion of the iron surface during firing at

700 °C. This phenomenon was also reported by S.K. Yen in 316 SS coated with ZrO<sub>2</sub>.<sup>11</sup> As shown in Figure 5d, a flat area of the coated electrode appears like the uncoated area (see Figure 5a). However, this flat area still has enough TiO<sub>2</sub> on the surface to be detected by EDX analysis.

After several cyclic voltammograms were obtained, the surface exposed to the test solution was damaged. In Figure 5e, cracks and delamination of the surface can be observed. EDX analysis of the different areas shows that the TiO<sub>2</sub> film was not present in the areas of delamination, while only iron and the minor components are present inside these areas. Although further studies of titania coated stainless steel are being conducted, it does not appear that stainless steel supports will be suitable for this application.

### Stability and Activity of Titanium-Supported Photoelectrodes

SEM analysis of the titanium-supported photoelectrodes shows that the surface is irregular with particles of different sizes deposited in the depressions on the surface (see Figures 6a-b). After coating, these particles remain under the film of TiO<sub>2</sub> (see Figures 6c-d) and are associated with the formation of cracks on the film. SEM analysis of samples pre-treated in different ways indicated that the origin of the particles was the stainless steel polish used in the first step of the pretreatment procedure. In the next samples this step was eliminated. Figure 6e shows the surface of a sample pretreated only by sonication with acetone in an ultrasonic bath for 5 h (with the bath cycled on and off for periods of 15 min) and coated first with a layer of alcohol-based sol (fired at 450 °C for 1 h) and then one layer of dialyzed aqueous-based sol (fired at 400 °C for 5 h). Notice that this second method for pretreating electrodes does not cause particles to deposit on the electrodes. However, cracks in the coating still could not be avoided. These cracks do not appear to be associated with particles deposited in surface depressions but appear to result from contraction of the coating after the firing procedure. These observations may indicate that these coatings are too thick to adhere well to the titanium electrode.

In another experiment, four plates of titanium were polished with an aqueous suspension of 0.3 μm Al<sub>2</sub>O<sub>3</sub> particles. Two plates were coated with three layers of a dialyzed aqueous TiO<sub>2</sub> sol, after which one was fired at 300 °C for 5 h and the other at 500 °C for 5 h. One of the uncoated plates was fired at 300 °C and the other at 500 °C. The films and the surfaces were characterized by X-ray diffraction (XRD, Table 1) and SEM (Figures 7a-f).

Figures 7a and 7b show the surface of uncoated and coated samples fired at 300 °C respectively. By comparing these figures, one can conclude that the TiO<sub>2</sub> film covers completely the surface of the support. The coated sample exhibits a homogeneous surface with small pores and some cracks in the coating. Images of the uncoated (Figure 7c-d at different magnifications) and coated (Figures 7e-f at different magnifications) samples fired at 500 °C are also shown. Once again, the film covers completely the surface of the metal. However, after firing at 500 °C the particles of TiO<sub>2</sub> are well defined and bigger than when

fired at 300 °C. As shown in Table 1, this growth in particle size is also associated with partial conversion of anatase crystals to rutile.

Table 1 Crystal structures of the surfaces of titanium plates treated in different ways.

	Fired at 300 °C	Fired at 500 °C
Uncoated	No Crystalline Phase	Rutile
Coated	Anatase	Anatase + Rutile

TiO<sub>2</sub> supported on titanium displays both photoelectrocatalytic activity and reasonable stability. Figure 8 shows the average activity of individual photoelectrodes that were fired at different temperatures, with the error bars representing the relative standard deviation observed in either three or four tests of each electrode. While the electrode that was fired at 300 °C was not the most active, it did display the best reproducibility. Figure 9 indicates the variation in behavior that was observed for this electrode.

On the other hand, for the electrode that was fired at 500 °C, a continuous diminution in its catalytic activity was noticed as each of the three tests was conducted. After the tests were completed, photomicrographs of the photoelectrodes fired at 500 °C indicated that in some areas the film of TiO<sub>2</sub> had separated from the substrate. The lack of contact between the titania coating and the conductive substrate may contribute to the decreased activity of this photoelectrode. However, the current that passes through the reactor is higher for the electrode fired at 500 °C (2.8-3.5 mA) than for the electrode fired at 300 °C (1.6-2.0 mA). In addition, it appears that the particles in the titania coating fired at 500 °C are larger than the particles in the titania coating fired at 300 °C. Thus, the larger particles improve the conductivity of the photoelectrodes. This behavior is not surprising. As the porous coatings are heated, grain growth will occur. As the particle size increases, the number of grain boundaries decreases. Because each grain boundary resists the passage of current, the conductivity of the coatings, and thus of the photoelectrodes, should increase with increasing firing temperature.

However, coatings that contain larger particles do not display improved catalytic activity. In addition to the possible delamination of the TiO<sub>2</sub> film mentioned above, two other factors may also contribute to this behavior. i) XRD analysis of the films indicates that the crystal structure of the films fired at 300 °C is that of the anatase form of titania, while the films fired at 500 °C are a mixture of anatase and rutile. Results from several photocatalytic studies have suggested that rutile is the less photoactive form of titania. ii) Firing these porous coatings at higher temperatures reduces their surface area. Thus less catalyst will contact the test solution in the coatings that were fired at 500 °C. Both of these factors would offset the improvement in conductivity that is obtained by firing the coatings at 500 °C. Because the titania-coated titanium electrodes displayed reasonably reproducible behavior in these initial tests (as opposed to the significant degradation of the

other substrates that was observed), further tests of the photocatalytic and photoelectrocatalytic properties of these titanium-supported photoelectrodes were conducted. These additional tests are described in the next section, using coatings of titania deposited from dialyzed aqueous sols.

### Effect of Different Variables on the Behavior of the Titanium-Supported Photoelectrodes

#### a) Effect of the Applied Potential

The effect of the applied potential on the removal of formic acid using photoelectrodes fired at different temperatures (i.e, the photoelectrocatalytic process) is shown in Figures 10a and 10b. We believe that these results correspond to the photoelectrochemical process because the pure electrochemical oxidation of formic acid on TiO<sub>2</sub> films deposited on conductive glass occurs only at potentials higher than 2 V<sup>12</sup> and on uncoated titanium at potentials higher than 3 V (this work).

Inspection of Figures 10a and 10b indicates that, for films fired at both 300 and 500 °C, the degradation of formic acid is highest for applied potentials of +1.0 V. However, only a small improvement in degradation ability is obtained by increasing the applied potential from +0.5 to +1.0 V. Therefore further studies were conducted under an applied potential of +0.5 V.

#### b) Effect of the Number of Layers of TiO<sub>2</sub>

Photoelectrodes containing various numbers of layers of dialyzed aqueous TiO<sub>2</sub> were fabricated. Figure 11 shows the activity of these photoelectrodes after being used for three hours of treatment. The amount of formic acid degraded is roughly proportional to the amount of deposited on the substrate (see Figure 12). The data shown in Figure 11 demonstrate several trends. 1) Application of a potential of +0.5 V across the titania coating significantly increases the activity of the photoelectrode above that observed when no potential is applied. 2) With a potential of +0.5 V applied across the photoelectrode, only a relatively small improvement in the activity of the photoelectrode is observed when more than two layers of titania are present. 3) Application of a potential across the titania coating has only a small effect when the coating consists of 10 layers of titania. Fluctuations in the amount degraded with different numbers of layers were reported previously in experiments that employed TiO<sub>2</sub> supported on conductive glass photoelectrodes.<sup>13</sup> These fluctuations were attributed to experimental variations. The first observation can be explained readily. When titania is illuminated by band gap radiation, electron-hole pairs are generated that are responsible for the photocatalytic activity of the material. By applying a potential across the photoactive titania, recombination of photogenerated electron-hole pairs is minimized. As a result the activity of the titania increases. Note that other factors may well contribute to this phenomenon which has been reported by several researchers.<sup>14-19</sup> There is also an obvious explanation for the other two observations reported above. Because titania is a poor conductor of electrical current, the thicker coatings of titania that are formed by depositing more layers of titania on the substrate are likely to inhibit the effectiveness of the applied electric field. In these experiments, though, a second factor may well contribute. If the degradation of formic acid follows first order kinetics, then the removal of additional

formic acid beyond the 60% removed by two layers of  $\text{TiO}_2$  may proceed slowly. These experiments were not conducted in a manner that would allow these two possibilities to be distinguished.

The activity of multilayer photoelectrodes was observed to decrease with the number of times that they were used. For example, when the photoelectrode that was coated with 4 layers of titania was employed in three successive tests, the activity of the photoelectrode decreased by 22% as these tests were conducted. SEM analysis of this photoelectrode indicates that the diminution in its activity could not be associated with delamination of the  $\text{TiO}_2$  layer. However, the mass of the photoelectrode was found to decrease by 0.9 mg after it was used three times. Therefore, it appears that the stability of titanium-supported photoelectrodes that contain multiple layers of titania is questionable.

#### c) Effect of the Concentration of NaCl

Figure 13 shows the effect of different concentrations of NaCl in solution on the activity of the titanium-supported  $\text{TiO}_2$  coated photoelectrodes. The presence of NaCl seems to decrease the rate of degradation of formic acid in the pure photochemical process. This phenomenon was reported previously in studies of photocatalysis<sup>20</sup> and in a study of photoelectrocatalysis that employed titania photoelectrodes coated on conductive glass.<sup>13</sup> Lowered efficiencies in photocatalytic reactions with increasing ionic strength are likely attributable to the competition between the formate ion and electrostatically adsorbed ionic species at the  $\text{TiO}_2$  surface. Application of a positive potential not only improves the activity of the titania photocatalyst but also minimizes the effect of the added NaCl. At present the reason for this improved performance is not clear.

### SUMMARY

$\text{TiO}_2$  supported on metals displays photocatalytic and photoelectrocatalytic activity, but the stability of the photoelectrodes depends on the stability of the metal against corrosion. In spite of the efforts made to date, films of  $\text{TiO}_2$  can not prevent the corrosion of copper, aluminum or stainless steel. Such corrosion may also occur on  $\text{TiO}_2$  coated titanium electrodes, but this possibility has not been proven.  $\text{TiO}_2$  coated titanium electrodes have been shown to display reproducible behavior with repeated use in photoelectrocatalytic processes. Thus, this system has been studied most extensively for this project.

Purely photocatalytic activity seems to vary with the support. For example, the photoactivity of  $\text{TiO}_2$  supported on stainless steel is lower than the photoactivity of  $\text{TiO}_2$  supported on titanium or aluminum. However, exposure of  $\text{TiO}_2$  coated aluminum electrodes to near UV light and a saline solution of formic acid causes severe corrosion of these electrodes.

Application of positive potentials across  $\text{TiO}_2$  films supported on titanium improves the efficiency of the photocatalytic process. This behavior is the same as previously reported with  $\text{TiO}_2$  supported on conductive glass. Firing temperature plays an important role in determining the electrochemical behavior of the electrodes. The intensity of the

current in the system (under otherwise identical conditions) increases with the firing temperature, although no corresponding improvement in the catalytic activity was detected. Catalytic activity of these electrodes can be increased by applying multiple coatings of TiO<sub>2</sub> to the titanium electrode. However, more studies are necessary in order to improve the adherence of multilayer TiO<sub>2</sub> electrodes with repeated use. We expect to find an optimal thickness for the film of TiO<sub>2</sub> that provides maximum photocatalytic activity with the minimum amount of TiO<sub>2</sub> when a positive potential is applied across the electrode.

The application of positive potentials across TiO<sub>2</sub> films diminishes the adverse effect of salt in solution on the photocatalytic activity of the system. This result is very interesting because most aqueous wastes that could be purified using this technology contain some salt.

### Electrochemical Studies

This aspect of the work is pertinent to a DOE interest in energy conversion devices. One approach to the useful conversion of sunlight into electrical energy employs wide band gap semiconductors such as titania. These compounds tend to be more stable to oxidation by air and water than small band gap semiconductors such as Si, InP, and GaAs.<sup>21</sup> However, photoelectrodes made from wide band gap materials must be sensitized with dyes or with high concentrations of dopants in order to extend their wavelength responses into the visible region of the solar spectrum. In a particularly exciting development, Grätzel and co-workers have developed efficient photoelectrochemical cells through the use of sensitizers based on transition metal complexes deposited on nanocrystalline titanium dioxide electrodes.<sup>22-27</sup>

The highest efficiency reported to date for such systems has been obtained using nanocrystalline TiO<sub>2</sub> coated with [Ru(II)(4,4'-(CO<sub>2</sub>H)<sub>2</sub>-2,2'-bipyridine)<sub>2</sub>(NCS)<sub>2</sub>] (abbreviated herein as (Ru(H<sub>2</sub>L')<sub>2</sub>(NCS)<sub>2</sub>), where L' is 4,4'-dicarboxylato-2,2'-bipyridine), for which overall solar-to-electrical energy conversion efficiencies of up to 10% have been reported.<sup>24</sup> Notably, the (Ru(H<sub>2</sub>L')<sub>2</sub>(NCS)<sub>2</sub>) complex requires excitation by 2.5 eV photons before significant light absorption takes place. In addition, the redox potential of (Ru(H<sub>2</sub>L')<sub>2</sub>(NCS)<sub>2</sub>)<sup>+0</sup> is ~ 0.5 V more positive than the redox potential of the I<sup>-</sup>/I<sub>3</sub><sup>-</sup> system that is used to carry the faradaic charge in the electrolyte. Consequently, changes in the sensitizer that extend its light absorption to lower energies while maintaining the excited state redox potential at the same energy level relative to the TiO<sub>2</sub> can yield improved efficiencies, provided that such changes do not produce concomitant decreases in the open-circuit voltage and/or the fill factor of the resulting photoelectrochemical device.

This strategy has been explored by a few researchers, with limited success to date.<sup>23,25-30</sup> In this work, we have explored the approach of replacing ruthenium with osmium in the transition metal complexes that are used to sensitize nanocrystalline TiO<sub>2</sub>. The osmium complexes are expected to have an additional absorption band at longer wavelengths compared to a ruthenium complex having the same ligands, because direct

excitation to the triplet state in Os(II) (bipyridine)<sub>x</sub>L<sub>y</sub> systems is not as forbidden as in the Ru(II) (bipyridine)<sub>x</sub>L<sub>y</sub> systems.<sup>31</sup> Higher photocurrents are therefore expected for TiO<sub>2</sub> electrodes coated with the osmium complexes, provided that the excited state in the Os complex effectively injects electrons into the TiO<sub>2</sub> support.

The Os complexes have other potential advantages relative to their Ru analogs. Although the excited-state lifetimes for Os complexes are typically shorter than those for the analogous Ru complexes, the Os(II) excited state should be as effective as the Ru(II) species in sensitizing TiO<sub>2</sub> because electron injection into nanocrystalline TiO<sub>2</sub> is thought to occur on a sub-picosecond timescale.<sup>32-36</sup> Perhaps more importantly, the ground-state potential of the Os complexes can be readily tuned to less positive potentials by using stronger donor ligands.<sup>37</sup> By using a sensitizer with a less positive ground state redox potential and a constant excited state redox potential, less energy will be wasted in the reduction of Os(III) to Os(II) by iodide, possibly yielding even further improvements in the efficiency of the overall system. However, it is not clear whether the ground states of the Os(III) dyes will have sufficient driving force to oxidize iodide at a rate rapid enough to support the required current density between the electrodes in the cell under typical solar illumination conditions. We have therefore performed electrochemical experiments to determine both the ground and excited state redox potentials of the Os and Ru complexes in order to probe the device performance as a function of the position of these energetic parameters.

Finally, if the dominant back reaction in all cases is reduction of I<sub>2</sub>, as has been proposed to be the rate-determining process in the specific case of Ru(H<sub>2</sub>L')<sub>2</sub>(NCS)<sub>2</sub> as the sensitizer for nanocrystalline TiO<sub>2</sub> electrodes,<sup>24</sup> one would expect that the photovoltage would remain relatively constant at a constant carrier injection level, regardless of which dye is used to generate the injected electrons into the TiO<sub>2</sub> support. Use of a series of dyes (Scheme II) has allowed us to probe the generality of this hypothesis in order to better understand the factors that control the photovoltage of dye-sensitized nanocrystalline TiO<sub>2</sub>/CH<sub>3</sub>CN contacts.

We observed that replacing the ruthenium metal center of polypyridine complexes with osmium extended the light absorption and spectral response of nanocrystalline TiO<sub>2</sub> photoelectrodes to lower wavelength values without sacrificing significant photoelectrochemical energy conversion performance. The Os complexes thus seem very promising candidates for further optimization in operating photoelectrochemical cells for solar energy conversion applications. The ground state potential of Os(H<sub>2</sub>L')<sub>2</sub>(NCS)<sub>2</sub> (0.4 V vs. SCE) offers a lower limit for the ground-state redox potential of the dye in the current configuration of the electrochemical cell and redox couple. Finally, for electrodes with very low dye coverages, the open-circuit photovoltage was mainly determined by the reduction of I<sub>2</sub>, whereas a more complicated mechanism is apparently operative for electrodes having higher dye coverages.

In addition, we have studied the electron transfer dynamics in solar cells that utilize sensitized nanocrystalline titanium dioxide photoelectrodes and the iodide/triiodide redox

couple on a nanosecond time scale. The ruthenium and osmium bipyridyl complexes  $\text{Ru}(\text{H}_2\text{L}')_2(\text{CN})_2$ ,  $\text{Os}(\text{H}_2\text{L}')_2(\text{CN})_2$ ,  $\text{Ru}(\text{H}_2\text{L}')_2(\text{NCS})_2$ , and  $\text{Os}(\text{H}_2\text{L}')_2(\text{NCS})_2$ , where  $\text{H}_2\text{L}'$  is 4,4'-dicarboxylic acid 2,2'-bipyridine, inject electrons into the semiconductor with a rate constant  $> 10^8 \text{ s}^{-1}$ . The effects of excitation intensity, temperature, and applied potential on the recombination reaction were analyzed using a second-order kinetics model. The rates of charge recombination decrease with increasing driving force to the oxidized sensitizer, indicating that charge recombination occurs in the Marcus inverted region. The electronic coupling factors between the oxidized sensitizer and the injected electrons in the  $\text{TiO}_2$  and the reorganization energies for the recombination reaction vary significantly for the different metal complexes. The charge recombination rates are well-described by semiclassical electron transfer theory, and reorganization energies are 0.55–1.18 eV. Solar cells sensitized with  $\text{Ru}(\text{H}_2\text{L}')_2(\text{CN})_2$ ,  $\text{Os}(\text{H}_2\text{L}')_2(\text{CN})_2$ , and  $\text{Ru}(\text{H}_2\text{L}')_2(\text{NCS})_2$  have favorable photoelectrochemical characteristics and iodide is oxidized efficiently. In contrast, iodide oxidation limits the efficiency of cells based on sensitization of  $\text{TiO}_2$  with  $\text{Os}(\text{H}_2\text{L}')_2(\text{NCS})_2$ . The observation that charge recombination occurs in the Marcus inverted region has important implications for the design of molecular sensitizers in nanocrystalline solar cells operated under our experimental conditions. The data indicate that under our conditions sensitizers having more negative ground-state reduction potentials would lead to increased charge recombination rates, because of inverted region effects. Therefore, use of such systems would lead to increased back reaction rates that would, to some extent, counteract the increased photocurrent density produced by better overlap between the absorption spectrum of the sensitizer and sunlight. One approach to dealing with this issue is to modify the electronic coupling between the  $\text{TiO}_2$  and the oxidized form of the sensitizer. In this fashion, charge recombination could be minimized while allowing sensitizer regeneration to be facile. Controlling the surface charge, increasing the distance between the metal center and the semiconductor, and employing molecular dyad sensitizers are possible ways to achieve these goals. Our findings serve as a benchmark for evaluating the success of these various approaches in the design of sensitizer/ $\text{TiO}_2$  combinations that have improved solar energy conversion properties.

Electrodes were characterized both in the dark, to determine their baseline electrochemical properties, and in the light with adsorbed dyes, in order to determine their trap state density and other properties that will be important in ultimately affecting the performance of these systems in an electrochemical cell. These studies are described briefly below.

Electrodes were prepared by first depositing a layer of  $\text{TiCl}_4$  in isopropanol onto 3 mm thick glass coated with a conducting layer of F-doped  $\text{SnO}_2$ . The layer was evenly spread by pulling a glass slide across the surface of the electrode, where Scotch tape on either side of the electrode region acted as a spacer for the slide. After the isopropanol had evaporated, the colloid solution was spread onto the conducting glass in a similar fashion. Once this layer had dried, the electrodes were fired in a tube furnace under flowing air at  $450^\circ\text{C}$  for 30 minutes. Once the electrodes had cooled, 100 mL of a freshly made solution of 0.2 M  $\text{TiCl}_4$  in water was deposited on each electrode. After the electrodes were

covered and allowed to sit overnight, the electrodes were rinsed with isopropanol. Sample electrode thicknesses were approximately 5  $\mu\text{m}$  as measured by profilometry.

Initial experiments with  $\text{TiO}_2$  electrodes showed poor reproducibility. It was hypothesized that variables such as water concentration and solution pH were affecting the current-voltage behavior of these electrodes, so care was taken to control these variables. All reagents and solutions listed above were stored in a nitrogen-purged box after purification. The pyridinium triflate and pyridinium were added to both the dye and electrolyte solutions in 0.001 M concentrations to maintain a constant initial pH. In pH studies, these buffered solutions were made more basic by adding Proton Sponge. Enough Proton Sponge was added so that the pyridine/pyridinium could no longer act as a buffer. All cells were constructed inside the nitrogen-purged box and sealed to avoid water contamination before being brought out of the box. These precautions led to greatly improved reproducibility.

Current density vs potential experiments were performed using an EG&G Princeton Applied Research (PAR) Model 362 Potential Controller in conjunction with a Houston Instrument Omnigraphic 2000 recorder. Light intensities were controlled by the use of an ELH W-halogen bulb and were determined by use of a calibrated silicon photodiode (Solarex). A UV filter was used to avoid direct excitation of electrons in the titanium dioxide. All measurements were performed in a three-electrode potentiostatic set-up, with a Pt wire reference and Pt gauze counter electrode. The distance between the working and counter electrodes was approximately 2 mm and no stirring was performed.

Some dye-electrolyte combinations were found to require some equilibration time to reach a stable open-circuit voltage; therefore, all cells were allowed to equilibrate for at least 30 minutes after exposure to a new solution before data published here were recorded. After exposure to Proton Sponge, electrodes were allowed to reequilibrate with the buffered  $\text{I}^-/\text{I}_2$  solution for at least 2 hours. Although the current-voltage properties of these junctions remained stable while the cell was assembled, once the electrodes were removed from the iodine solution they tended to degrade. For this reason, fresh electrodes were used in all experiments.

Spectral response data was obtained by biasing the cell to short circuit and measuring the voltage output from the current monitor on the potentiostat. Monochromatic light was obtained from a Spex 1682A tungsten lamp in conjunction with a Spex 1681B monochromator with 1.25 mm slits. For the  $\text{TiO}_2$  electrodes, the dark current tended to drift slightly over time, so the dark current was measured at each wavelength and subtracted from the photocurrent at that wavelength. The light intensity from a beam-split portion of the monochromator output was measured by monitoring the photocurrent at a Si photodiode from United Detector Technology. This diode thus served as a calibration of the lamp intensity. Quantum yields were obtained by placing a calibrated Si photodiode in the same position as the  $\text{TiO}_2$  working electrode and measuring the photocurrent at short circuit, then correcting the data from the  $\text{TiO}_2$ . Current-voltage data at 1 Sun illumination was obtained before and after each run. Electrodes which showed significant decreases in

photocurrent (>5%) were viewed to be defective and were not included in the final analysis.

## **Results:**

### **A. Characterization of Unsensitized Electrodes**

The current-voltage behavior in the dark for a nanoporous titanium dioxide electrode was first compared to the current-voltage behavior for a conducting glass electrode in a solution of  $\text{LiI}/\text{I}_2$ . Both reduction and oxidation of the  $\text{I}_2/\text{I}^-$  couple require high overpotentials at the conducting glass electrode and very low currents are observed in either potential direction. In contrast, the  $\text{TiO}_2$  electrode shows rectifying behavior and yields much higher dark currents in forward bias than the conducting glass alone. This behavior indicates there are slow kinetics of electron transfer for iodine at the conducting glass surface. Since the  $\text{TiO}_2$  is capable of reducing  $\text{I}_2$  but not of oxidizing  $\text{LiI}$  in the dark, a concentration gradient is developed which effectively separates the charge. To further support this explanation, a similar experiment was performed with  $\text{Me}_2\text{Fc}^{+/0}$  as the redox couple in solution. This redox couple was chosen because the reduction potential of this couple is reasonably close to that of the  $\text{I}_2/\text{I}^-$ . In this case, very high currents were observed in both potential directions at the conducting glass electrode. At the titanium dioxide electrode, similar behavior was observed. Although data is not shown here, dye-sensitized electrodes immersed in solutions of  $\text{Me}_2\text{Fc}^{+/0}$  developed no observable photovoltages and showed no photocurrent at short circuit.

### **B. Spectral Response**

Spectral response data for electrodes sensitized with the dyes were also obtained, in order to characterize the grain boundary transport processes through the  $\text{TiO}_2$  electrodes. The results can be explained fully by three coinciding factors. First, as expected, the spectral response roughly correlates with the absorption spectrum of each dye. Dyes which have lower extinction coefficients such as the  $\text{RuL}'_3$  and  $\text{OsL}'_3$  showed lower current responses. The wavelength at which the maximum photocurrent was observed corresponded to the absorption maximum for each dye. Second, within a given set of ligands, the osmium dyes showed much more photocurrent at higher wavelengths. This phenomenon is due to the weak band present in the absorption spectra of the osmium dyes which is not present in the ruthenium dyes and which likely arises due to the population of triplet states in the osmium dyes. The only response which cannot be explained by a combination of these two effects is that of electrodes sensitized with the  $\text{OsL}'_2(\text{SCN})_2$  dye. This dye shows very high light absorption, yet electrodes sensitized with this dye show very poor energy conversion. However, this effect can be explained by examining the ground state reduction potentials of the dyes. Of the dyes examined in this work, the  $\text{OsL}'_2(\text{SCN})_2$  has the least positive reduction potential and in fact is only 0.18 V positive of the  $\text{I}_2/\text{I}^-$  redox couple. It is likely, therefore, that the smaller driving force for regeneration of the dye limits the efficiency of this dye.

### **C. Effect of pH on the $\text{TiO}_2$ Electrochemistry**

TiO<sub>2</sub>/RuL'<sub>2</sub>(SCN)<sub>2</sub> electrodes were characterized as a function of Proton Sponge concentration. In initial sets of experiments, each electrode was first characterized in a solution containing only buffered LiI/I<sub>2</sub>. When Proton Sponge was added, the open circuit voltages increased dramatically and the short circuit currents dropped. This effect is believed to be due to a shifting in the band edge position of the TiO<sub>2</sub> with pH. As the difference between the conduction band edge position of the TiO<sub>2</sub> and the reduction potential of the LiI/I<sub>2</sub> is increased, the open circuit voltage gets larger. If the conduction band edge becomes so negative that the excited dye cannot inject electrons efficiently, the short-circuit current density decreases. However, when the electrode was reintroduced to the buffered solution, the open-circuit voltages decreased as expected, but the short-circuit current densities did not recover.

As mentioned above, once the electrodes were exposed to iodine solution, the removal of the iodine contact caused some irreversible degradation of the electrode which could account for the change between the first and last potential scan. To determine whether the decrease in current upon exposure to Proton Sponge was completely due to emptying the cell and refilling it, current-voltage curves of fresh TiO<sub>2</sub>/RuL'<sub>2</sub>(SCN)<sub>2</sub> electrodes in solutions containing various concentrations of Proton Sponge were examined. The results for the 10 mM Proton Sponge solution were almost identical to those of electrodes first exposed to buffered solution. Since the dyes are known to desorb in aqueous base, the more basic solutions could cause some loss of dye even in non-aqueous solutions, resulting in lower currents when the electrodes are reimmersed in buffered solution. Although this effect may also account for part of the current decrease, the voltage increases in basic solution cannot be explained by a loss of dye, thus a band edge shift seems likely. The dark curves for this dye-electrode system show a similar shift in the voltage, further supporting the presence of a band edge shift.

#### **D. Effect of pH on Luminescence of the Adsorbed Dye- TiO<sub>2</sub>/RuL'<sub>3</sub> Electrodes:**

The effect of pH on the TiO<sub>2</sub> band edge positions was further examined through luminescence studies of the adsorbed dye. If a shift in the band edge position causes a decrease in the injection rate constant, resulting in a decrease in photocurrent increase, the quantum yield for luminescence should increase, and thus luminescence intensity should increase as the pH is increased. If the decrease in current observed above was solely due to a loss of dye, the luminescence intensity should decrease due to the smaller amount of dye on the surface of the electrode. Luminescence studies were first attempted on TiO<sub>2</sub>/RuL'<sub>2</sub>(SCN)<sub>2</sub> electrodes, but the luminescence intensity was very low and the peak was at a wavelength too positive to detect with the system available. TiO<sub>2</sub>/RuL'<sub>3</sub> electrodes were chosen as an alternate because of the strong luminescence of the L'<sub>3</sub> dyes. When Proton Sponge is present, the luminescence intensity increases, as expected. After 2 hours of immersion in the buffered solution after exposure to the Proton Sponge solution, the luminescence drops back down near the initial value. To minimize the effects of changing solutions, the luminescence experiment was repeated with a new electrode in a CH<sub>3</sub>CN solution containing 0.001 M/0.001 M pyridine/pyridinium. In this case, a few drops of

glacial acetic acid were then added to the solution to neutralize the Proton Sponge. An immediate decrease in the luminescence intensity was observed, consistent with an increased dye injection efficiency and a positive conduction band edge shift due to the decreased pH.

To make sure the effect of pH on the current-voltage characteristics was not limited to the  $\text{RuL}'_2(\text{SCN})_2$  system, current-voltage curves of the  $\text{TiO}_2/\text{RuL}'_3$  electrodes were examined as a function of pH. The photocurrents dropped significantly when the Proton Sponge concentration was changed from 0 to 0.010 M. The large amount of hysteresis present makes it difficult to quantify the open-circuit voltage change although it appears to increase slightly. As in the previous case, the photocurrents decrease from their initial value on reimmersion and equilibration with the buffered solution. The dark curves show a large negative shift in the voltage when the electrode is exposed to Proton Sponge, similar to the behavior observed with the  $\text{TiO}_2/\text{RuL}'_2(\text{SCN})_2$  electrodes. The dark curves return to their previous position when the electrode is reimmersed in the buffered solution.

### **E. Summary and Conclusions**

The data collected in this project appear to provide a rational approach for design of more efficient nanoporous electrodes. As discussed above, the first requirement for this type of system is slow charge transfer kinetics between the back contact of the electrode and the sacrificial electron donor/acceptor in solution. This condition allows the separation of charge by a diffusion gradient rather than drift. A similar approach has been used in single crystal systems such as Si, in which ohmic selective back contacts were used in conjunction with Si electrodes with very high carrier lifetimes to produce efficient solar cells.

The effect of solution pH on the interfacial energetics of the junction should be considered. The data demonstrate that changing the solution pH can have a profound effect on the current-voltage properties of the cell even in nonaqueous solutions. Increasing the pH has been shown to result in photovoltage increases of up to 200 mV. Again, though, this parameter needs to be optimized for the system studied. Studies of the effects of these properties on the electrochemistry of aqueous systems, and a comparison of the behavior of undoped and Nb-doped  $\text{TiO}_2$  electrodes, are being performed at present.

In addition, a series of osmium polypyridyl complexes having various ground state reduction potentials has been synthesized and used to sensitize nanoporous titanium dioxide electrodes to solar illumination. The spectral response and current vs. potential properties of electrodes modified with these dyes have been compared with the behavior of their ruthenium analogs. The trends can be explained by the differences in absorption spectra and ground state redox potentials. The osmium complexes appear to be promising candidates for further optimization in operating photoelectrochemical cells for solar energy conversion applications. Of the materials studied, all complexes having ground-state redox potentials in methanol more positive than  $\sim 0.4$  V vs. aqueous SCE were able to sustain oxidation of  $\text{I}^-/\text{I}_3^-$  with a high steady-state quantum yield. For electrodes with very low dye

coverages, the open-circuit voltage was mainly determined by the rate of reduction of  $I_2$ , whereas for high dye coverages, the open-circuit voltage depended on the nature of the complex and on the dye loading level.

## FIGURE CAPTIONS

**Figure 1.** Scanning electron photomicrographs of aluminum photoelectrodes fired at 500 °C and treated in different ways. a) Titania coated electrode prepared as described in the text before exposure to the test solution. b) Same electrode as (a) after 7 h exposure to the test solution and UV light with pure oxygen bubbled through the solution. c) Uncoated electrode after 8 h exposure to the test solution and UV light with pure oxygen bubbled through the solution.

**Figure 2.** Scanning electron photomicrograph of a 304 stainless steel-supported titania photoelectrode. The coating is the narrow band across the center of the figure that is labeled 79.4 nm. The relatively uniform grayish area below the coating is the stainless steel electrode, while the region above the coating is a layer of resin used to prepare the specimen.

**Figure 3.** Current-potential plot for a stainless steel-supported titania photoelectrode that was coated with 3 layers of alcohol-based titania sol and fired at 500 °C for 5 h.

**Figure 4.** Scanning electron photomicrographs of stainless steel photoelectrodes prepared in different ways. All samples were initially fired at 450 °C for 2 h. a) Uncoated electrode fired a second time at 500 °C for 5 h. b) Same as (a) but at higher magnification. c) Electrode coated with 3 layers of alcohol-based titania sol and fired at 500 °C for 5 h. d) Same as (c) but at higher magnification. e) Electrode coated with 1 layer of dialyzed aqueous-based titania sol and fired at 500 °C for 5 h. f) Same as (e) but at higher magnification. g) Electrode coated with 1 layer of peptized (80 °C) aqueous-based titania sol and fired at 500 °C for 5 h. h) Same as (g) but at higher magnification.

**Figure 5.** Scanning electron photomicrographs of stainless steel photoelectrodes. All samples were initially fired at 450 °C for 2 h. a) Uncoated electrode fired a second time at 700 °C for 5 h. b) Electrode coated with 1 layer of peptized titania sol and fired at 700 °C for 5 h. c) Magnification of the main feature shown in (b). d) Magnification of a flat area shown in (b). e) Coated surface prepared as in (b) after 50 cyclic voltammograms (-0.5 V to +0.5 V at a scan rate of 20 mV sec<sup>-1</sup>).

**Figure 6.** Scanning electron photomicrographs of titanium photoelectrodes prepared in different ways. a) Uncoated electrode pretreated as described in the text (see p. 2). b) Same as (a) but at higher magnification. c) Electrode coated with 1 layer of alcohol-based titania sol, fired at 450 °C for 1 h, coated again with 1 layer of dialyzed titania sol, and fired at 300 °C for 5 h. d) Same as (c) but at higher magnification. e) Electrode coated and fired as described in the text. Unlike the electrode shown in (a-d), this electrode has not been polished.

**Figure 7.** Scanning electron photomicrographs of titanium electrodes prepared in different ways. a) Uncoated electrode polished with alumina and fired at 300 °C for 5 h. b) Polished electrode coated with 3 layers of dialyzed titania sol and fired at 300 °C for 5 h. c)

Uncoated electrode polished with alumina and fired at 500 °C for 5 h. d) Same as (c) but at higher magnification. e) Polished electrode coated with 3 layers of dialyzed titania sol and fired at 500 °C for 5 h. f) Same as (e) but at higher magnification.

**Figure 8.** Effect of firing temperature on the photoelectrocatalytic activity of titanium-supported titania photoelectrodes. Electrodes were prepared by polishing titanium plates with stainless steel polish, coating with 1 layer of alcohol-based sol, firing at 450 °C for 1 h, coating with 1 layer of dialyzed titania sol, and firing at the indicated temperature for 5 h. Activity of the electrodes was measured as described in the text with an applied potential of +0.5 V. The percent of formic acid remaining in solution corresponds to the average of at least three separate tests.

**Figure 9.** Variation in activity of the titanium-supported titania photoelectrode that was fired at 300 °C.

**Figure 10.** Effect of applied potential on the removal of formic acid. a) Electrode prepared as described in Figure 8 and fired at 300 °C for 5 h. b) Electrode prepared as described in Figure 8 and fired at 500 °C for 5 h.

**Figure 11.** Activity of photoelectrodes both with and without an applied potential as a function of the number of layers of dialyzed titania sol applied to the electrode. All electrodes were first coated with 1 layer of alcohol-based titania sol and fired at 450 °C for 1 h. After the indicated number of coatings with the dialyzed sol, all electrodes were fired at 300 °C for 5 h.

**Figure 12.** Amount of titania deposited on the titanium support as a function of the number of layers of titania applied. Layer 1 includes the mass of both one coating of alcohol-based titania sol fired at 450 °C and one coating of dialyzed aqueous-based titania sol fired at 300 °C. Additional layers include the mass deposited from additional coatings of the dialyzed sol fired at 300 °C.

**Figure 13.** Effect of applied potential and salt concentration in the test solution on the activity of titania photoelectrodes. All electrodes were prepared by polishing titanium plates with stainless steel polish, coating with 1 layer of alcohol-based titania sol, firing at 450 °C for 1 h, coating with 1 layer of dialyzed titania sol, and firing at 300 °C for 5 h. (NAP = no applied potential).

**Relevance, Impact, and Technology Transfer:**

- a. The new knowledge impacts the ability to develop a low temperature relatively benign technology to process waste streams for remediation.
- b. The new knowledge might produce significantly lower overall costs in remediation processes if it can be implemented on a large scale with success.
- c. The new knowledge applies basic concepts in electrochemistry and materials science, in the development of robust metal oxides, for use in electrochemically-based remediation schemes for liquid waste streams.
- d. The project has been disseminated to various individual through conferences, presentations, and publications. Students have been educated in the technology and colleagues and potential users have been notified of the advances in the area that have been made during the course of this work.
- e. Larger scale trials of preliminary scale-up tests would seem warranted to validate the laboratory results obtained during the course of this work.
- f. The project has greatly enhanced the scientific capabilities of the collaborating scientists in that it has intimately involved teaming of materials scientists/water chemists at the University of Wisconsin with electrochemists/inorganic materials chemists at Caltech throughout the project. This cross-pollination of ideas has enhanced significantly the scientific capabilities and experiences of both laboratory sites.
- g. This research has lead to a new understanding of the role of nontraditional electrode materials in effecting electrochemically-catalyzed transformations of importance to toxic waste remediation processing.
- h. The outcomes need to be validated in scale-up tests to evaluate their promise and problems when transitioned from the laboratory to the pilot plant scale.
- i. Both DOE and EPA have expressed interest in the project; additionally some aspects are of interest to Dow Chemical and to DuPont as they pertain to new markets for utilization of titania.

### **Project Productivity:**

The project accomplished basically all of its initial research goals, on schedule and on budget.

### **Personnel Supported:**

Funding supported about a dozen different people for various amounts of time over the entire length of the project. At the University of Wisconsin, total salary expenditures supported the equivalent of 1 undergraduate student hourly per year, 1 graduate student per year, and 1 professional staff person at 66% time over the project. No faculty salary was paid from this grant. At Caltech the grant supported an equivalent of one graduate student, one post-doctoral fellow, and partial faculty salary per year.

### **Publications:**

Roberto J. Candal, Walter A. Zeltner, and Marc A. Anderson, 1999. Titanium-Supported Titania Photoelectrodes Made by Sol-Gel Processes, *J. Environ.Eng.* **125**(10), 906-912.

Roberto J. Candal, Walter A. Zeltner, and Marc A. Anderson, 2000. Effects of pH and Applied Potential on Photocurrent and Oxidation Rate of Saline Solutions of Formic Acid in a Photoelectrocatalytic Reactor, *Environ.Sci. Technol.* **34**(16), 3443-3451.

Bryce P. Nelson, Roberto Candal, Robert M. Corn, and Marc A. Anderson, 2000. Control of Surface and Zeta Potentials on Nanoporous TiO<sub>2</sub> Films by Potential-Determining and Specifically Adsorbed Ions, *Langmuir* **16**(15), 6094-6101

Darius Kuciauskas, Michael S. Freund, Harry B. Gray, Jay R. Winkler, and Nathan S. Lewis, "Electron Transfer Dynamics in Nanocrystalline Titanium Dioxide Solar Cells Sensitized with Ruthenium or Osmium Polypyridyl Complexes," *J. Phys. Chem. B.*, **2000**, in press.

Genevieve Sauvé, Marion E. Cass, Stephen J. Doig, Iver Lauermaann, Katherine Pomykal, and Nathan S. Lewis, "High Quantum Yield Sensitization of Nanocrystalline Titanium Dioxide Photoelectrodes with cis-Dicyanobis-(4,4'-dicarboxy-2,2' -bipyridine)osmium(II) or Tris(4,4" -dicarboxy-2,2" -bipyridine)osmium(II) Complexes," *J. Phys. Chem B*, **2000**, *104*, 3488-3491.

Genevieve Sauvé, Marion E. Cass, Stephen J. Doig, Iver Lauermaann, Katherine Pomykal, and Nathan S. Lewis, "Dye Sensitization of Nanocrystalline Titanium Dioxide with Osmium and Ruthenium Polypyridine Complexes", *J. Phys. Chem. B*, **2000**, *104*, 6821-6736.

**Interactions:**

This work was mainly reported at the last three symposia on TiO<sub>2</sub> Photocatalytic Purification and Treatment of Water and Air. These conferences are the major clearing house for research in environmental applications of photocatalysis. DOE and EPA laboratory staff attend these meetings regularly. In addition, aspects of this work have been presented at meetings of the American Chemical Society and the Electrochemical Society.

**Transitions:**

We are currently utilizing some of the knowledge gained in our DOE project for a project sponsored by the American Water Works Association to treat perchlorate contamination in California ground waters. We believe that, with a modified reactor design, this technology would be ideal for treating DOE mixed waste remediation sites.

**Patents:**

No patents were filed during this time

**Future Work:**

Some electrochemical reactor design engineering would be needed to scale this reactor to a pilot-plant version. Electron transport limitations resulting from the placement of the counter electrodes in our bench-scale reactor may have limited the reaction rates in the system. A better design in which these electrodes are located with cylindrical symmetry is warranted. In addition, we are now fabricating flexible electrodes on metalized supports that should aid in scaling up this reactor. The next step would be to build a pilot-plant version of this reactor to use in an actual waste-treatment scenario.

**Literature Cited:**

- (1) Lawrence, W. E.; Surma, J. E.; Gervais, K. L.; Sasser, K. N.; M. D. Ryder, M.; Buehler, F.; Pillay, G. "Interim Report on the Electrochemical Organic/Complexant Destruction in Hanford Tank Waste Simulants," Westinghouse Savannah River Company, 1994.
- (2) Lawrence, W. E.; Surma, J. E.; Gervais, K. L.; Sasser, K. N.; Ryder, M. D.; Buehler, M. F.; Pillay, G. "Interim Report on the Electrochemical Organic/Complexant Destruction in Hanford Waste Simulants," 1994.
- (3) Hobbs, D. T. "Summary Technical Report on the Electrochemical Treatment of Alkaline Nuclear Wastes," Westinghouse Savannah River Company, 1994.
- (4) Hobbs, D. T. In *Chapter 12: Electrochemistry For A Cleaner Environment*; J. D. Genders and N. L. Weinburg, Eds.; Electrosynthesis Company, Inc.: East Amherst, New York, 1992.

- (5). M. A. Anderson, M. J. Gieselmann and Q. Xu, *J. Membrane Sci.*, **39**, 243 (1988).
- (6) C. J. Brinker and G. W. Scherer, *Sol-Gel Science: The Physics and Chemistry of Sol-Gel Processing*, Academic Press, New York (1990).
- (7). Q. Xu and M. A. Anderson, *J. Mater. Res.*, **6**, 1073 (1991).
- (8) Q. Xu and M. A. Anderson, *J. Am. Ceram. Soc.*, **77(7)**, 1939 (1994).
- (9) H. Y. Ha and M. A. Anderson, *J. Environ. Eng.*, 122, 217 (1996).
- (10) A. Fernandez, G. Lassaletta, V. M. Jimenez, A. Justo, A. R. Gonzalez-Eliphe, J. M. Henmann, H. Tahiri and Y. Ait-ichou; *Appl. Catal. B: Environ.*, **7**, 49 (1995).
- (11) S.K. Yen, *191th Meeting of the Electrochemical Soc.*, Montreal, May 1997.
- (12) A. Wahl, M. Ulmann, A. Carroy, B. Jermann, M. Dolata, P. Kedzierzawski, C. Chatelain, A. Monnier and J. Augustynski; *J. Electroanal. Chem.*, 396, 41, (1995).
- (13) D.H. Kim and M.A. Anderson; *J. Environ. Eng.*; 121, 590, (1995).
- (14) D. H. Kim and M. A. Anderson, *Environ. Sci. Technol.*, 28, 479, (1994).
- (15) K. Vinodgopal, S. Hotchandani and P. V. Kamat; *J. Phys. Chem.*, 97, 9040, (1993).
- (16) L. Bahadur and T. N. Rao, *J. Photochem. Photobiol. A: Chem*, 91, 233, (1995).
- (17) A. Hagfeldt and M. Grätzel, *Chem. Rev.*, 95, 49, (1995).
- (18) K. Vinodgopal, I. Bedja and P. V. Kamat, *Chem. Mater.*, 8, 2187, (1996).
- (19). K. Vinodgopal and P. V. Kamat, *Chemtech*, 26, 18, (1996).
- (20). a) G. K. Boschloo, A. Goossens and J. Schoonman, *J. Electrochem. Soc.*, 144, 1311, (1997). b) M. Abdullah, G. K. Low and R. W. Matthews, *J. Phys. Chem.*, 94, 6820, (1990).
- (21) Tan, M. X.; Laibinis, P. E.; Nguyen, S. T.; Kesselman, J. M.; Stanton, C. E.; Lewis, N. S. *Progr. Inorg. Chem.* **1994**, 41, 21.
- (22) O'Regan, B.; Grätzel, M. *Nature (London)* **1991**, 353, 737.
- (23) Grätzel, M.; Kalyanasundaram, K. *Curr. Sci.* **1994**, 66, 706.
- (24) Nazeeruddin, M. K.; Kay, A.; Rodicio, I.; Humphry-Baker, R.; Müller, E.; Liska, P.; Vlachopoulos, N.; Grätzel, M. *J. Am. Chem. Soc.* **1993**, 115, 6382.

- (25) Heimer, T. A.; Bignozzi, C. A.; Meyer, G. J. *J. Phys. Chem.* **1993**, *97*, 11987.
- (26) Argazzi, R.; Bignozzi, C. A.; Heimer, T. A.; Castellano, F. N.; Meyer, G. J. *Inorg. Chem.* **1994**, *33*, 5741.
- (27) Nazeeruddin, M. K.; Müller, E.; Humphry-Baker, R.; Vlachopoulos, N.; Grätzel, M. *J. Chem. Soc., Dalton Trans.* **1997**, 4571.
- (28) Nazeeruddin, M. K.; Péchy, P.; Grätzel, M. *Chem. Commun.* **1997**, *18*, 1705.
- (29) a) Alebbi, M.; Bignozzi, C. A.; Heimer, T. A.; Hasselmann, G. M.; Meyer, G. J. *J. Phys. Chem. B* **1998**, *102*, 7577. b) Farzad F.; Thompson, D.W.; Kelly, C.A.; Meyer, G.J. *J. Am. Chem. Soc.* **1999**, *121*, 5577. c) Vrachnou, E.; Graetzel, M.; McEvoy, A.J. *J. Electroanal. Chem.*, **1989**, *258*, 193. d) Nazeeruddin, M. K.; Humphry-Baker, R.; Grätzel, M.; Murrer, B. A. *Chem. Commun.* **1998**, 719.
- (30) Amadelli, R.; Argazzi, R.; Bignozzi, C. A.; Scandola, F. *J. Am. Chem. Soc.* **1990**, *112*, 7099.
- (31) Kalyanasundaram, K. *Photochemistry of Polypyridine and Porphyrin Complexes*; Academic Press: San Diego, 1992, pp 626.
- (32) Hannappel, T.; Burfeindt, B.; Storck, W.; Willig, F. *J. Phys. Chem. B.* **1997**, *101*, 6799.
- (33) a) Tachibana, Y.; Moser, J. E.; Grätzel, M.; Klug, D. R.; Durrant, J. R. *J. Phys. Chem.* **1996**, *100*, 20056. b) Tachibana, Y.; Haque, S. A.; Mercer, I. P.; Durrant, J. R.; Klug, D. R. *J. Phys. Chem. B*; **2000**; *104*, 1198.
- (34) Rehm, J. M.; McLendon, G. L.; Nagasawa, Y.; Yoshihara, K.; Moser, J.; Grätzel, M. *J. Phys. Chem.* **1996**, *100*, 9577.
- (35) Ferrere, S.; Gregg, B. A. *J. Am. Chem. Soc.* **1998**, *120*, 843.
- (36) Eichberger, R.; Willig, F. *Chem. Phys.* **1990**, *141*, 159.
- (37) Kalyanasundaram, K.; Nazeeruddin, M. K. *Chem. Phys. Lett.* **1992**, *193*, 292.

**Feedback:**

A very good program overall and good experience for the researchers involved with the science.

**Appendices:**

None.